

GENERATION OF DEM AND ORTHOIMAGES FROM SPOT HRS STEREO DATA WITHOUT USING GCP

Peter Reinartz, Rupert Müller, Manfred Lehner, Manfred Schroeder
German Aerospace Center (DLR), Remote Sensing Technology Institute
peter.reinartz@dlr.de

Commission I, WG I/5

Key words: SPOT HRS, direct georeferencing, orthoimages, DSM generation, accuracy analysis, boresight alignment

ABSTRACT:

The High Resolution Stereo (HRS) Scientific Assessment Program offered by the French space agency CNES and ISPRS, provided data sets from the SPOT stereo camera system (HRS) together with high precision ancillary data. Two test data sets from this program were evaluated: one is located in Germany, the other in Spain. The first goal was to derive orthoimages and digital surface models (DSM) from the along-track stereo data by applying the rigorous model with direct georeferencing and without ground control points (GCPs). For the derivation of DSM, the stereo processing software, developed at DLR for the MOMS-2P three line stereo cameras was used. As a first step, the interior and exterior orientation of the camera, delivered as ancillary data from positioning and attitude systems were extracted. A dense image matching, using nearly all pixels as kernel centers provided the parallaxes. The quality of the stereo tie points was controlled by forward and backward matching of the two stereo partners using the local least squares matching method. Forward intersection leads to points in object space which are subsequently interpolated to a DSM in a regular grid. DEM filtering methods were also applied and evaluations carried out differentiating between accuracies in forest and other areas. Additionally, orthoimages were generated from the images of the two stereo looking directions. The orthoimage and DSM accuracy was determined by using GCPs and available reference DEMs of superior accuracy (DEM derived from laser data and/or classical airborne photogrammetry). As expected the results obtained without using GCPs showed a bias in the order of 5 m – 20 m to the reference data for all three coordinates. By image matching it could be shown that the two independently derived orthoimages exhibit a very constant shift behavior. In a second step few GCPs (3-4) were used to calculate boresight alignment angles, introduced into the direct georeferencing process of each image independently. This method improved the absolute accuracy of the resulting orthoimages and DSM significantly.

1. INTRODUCTION

Along track stereo data of the HRS camera onboard SPOT 5 were provided by the French space agency CNES in the framework of the HRS Scientific Assessment Program to test their capability for DSM and orthoimage production. The derivation of digital surface models (DSM) from along track stereo data from space has been performed with the German MOMS-2P camera (Kornus et al. 2000, Müller et al. 2001), the Japanese/American ASTER sensor on TERRA (Toutin et al. 2001) and the new very high resolution (VHR) cameras like IKONOS and Quickbird (Toutin 2005). The first two have lower resolutions (15-18 meter pixel size) than the new HRS sensor, whereas the latter have pixel sizes of ~1 meter but have the disadvantage that the worldwide stereo coverage is very low. Therefore the HRS sensor is an interesting new sensor to acquire optical stereo pairs for larger regions with a sufficient spatial resolution to produce high quality DSM with accuracies similar to the SRTM X-Band DSM (Rabus et al. 2003), or even better (Reinartz et al. 2005).

The HRS sensor gives for the first time the opportunity to derive orthoimages and DSM without the use of GCPs. This is due to the fact that the ancillary information, especially the gyro/star tracker attitude and DORIS (Doppler Orbitography and Radiopositioning Integrated by Satellite) position data, provided with the image data, exhibit a very high accuracy in comparison to former sensor systems. The goal of this investigation is to analyze the accuracy of the products (DSM and orthoimage) derived without the use of GCPs and to check the improvement with the help of only few GCPs which are only used to determine “boresight alignment angles” to correct the orientation of the images individually.

2. TEST AREAS, HRS- AND REFERENCE DATA

Two HRS stereo pairs of the test site in Bavaria/Germany and Catalonia/Spain were evaluated. The German test area is a region of about 40 x 50 km² in the southeastern part of Bavaria. The elevations range from 400 to 2000 meters in a mostly hilly, post-glacial landscape including some lakes and also mountains of the German Alps. This selection allowed the comparison of the DSMs for different land surface shapes, including forest and steep terrain.

The ground reference data selected for this test site were the following (see also Fig.1):

1. Four regions have a DEM grid spacing of 5 meters and an overall size of about 5 km x 5 km, derived from airborne laser scanning, the height accuracy is better than 0.5 meter (RMSE).
2. One region (area of Inzell, total: 10 km x 10 km, 25 meter spacing) consists partly of laser scanner data (northern part). The height accuracy is better than 0.5 meter (RMSE). The southern part of the DEM was derived from contour-lines 1:10 000. The height accuracy is about 5 meter (RMSE) due to the mountainous area.
3. A large region (50 km x 30 km) is covered by a coarser DEM with 50 meter grid spacing and height accuracy of about 2 meters (RMSE), derived from aerial photogrammetry.
4. The exact locations of 81 GCP (fix points), from which 20 were used in these investigations.

The Spanish test site covers a region of about 50 x 60 km² in Catalonia including the city of Barcelona. The ground reference data for the Catalonian area, similar to the landscape of the Bavarian test site but including the Mediterranean coast, are the following (see also Kornus et al. 2006):

1. 32 color orthoimages (1:5000) with pixel size of 0.5 meter and accuracy better than 1 pixel (RMSE)
2. DEM with pixel spacing 15.0 meter and orthometric height accuracy of 1.1 meter (RMSE)

The HRS image data which were provided by SPOT IMAGE contain the following parts:

1. 4 sets of 8 bit panchromatic image data (size 12000 x 12000 pixel = 120 km across x 60 km along track) of the Bavarian and Catalonian test area from two viewing directions in TIF format
2. XML-files containing all additional information regarding time synchronization, position (DORIS), attitude (star sensors and gyros) and interior orientation
3. Text files containing information on the delivered data.

The data of Bavaria were acquired on October 1st 2002 with a sun elevation of 38° and nearly no clouds. The data of Catalonia were acquired on October 15th 2002 with a sun elevation of 39° and no clouds. The radiometric quality of the Catalonian images is superior to the Bavarian imagery, which was judged by the image matching process, since the point density is significantly denser than in the Bavarian data set. The HRS-data were received in July 2003. First results were presented at the ISPRS Congress in Istanbul in 2004 (Reinartz et al 2004, Müller et al 2004).

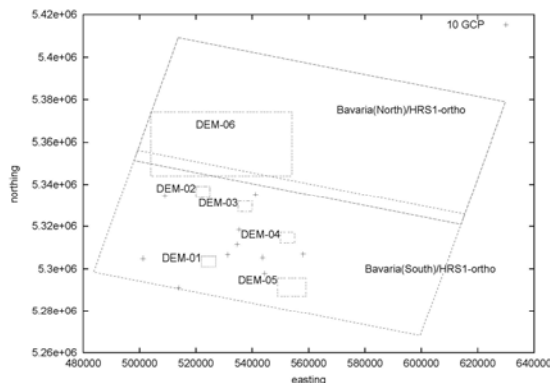


Figure 1. Location of the test areas at the most southeastern part of Germany, location of the SPOT-HRS scenes with DEM reference sites and some ground control points

3. PROCESSING OF THE ANCILLARY DATA

The delivered SPOT 5 HRS Level 1A product consists of the image data in standard TIF format and the metadata in DIMAP format. The following information was extracted for each image from the XML ancillary file for further processing:

1. Satellite ephemeris data containing position and velocity measured by the DORIS system every 30 seconds with respect to the ITRF90 (International Terrestrial Reference Frame 1990) system during the data take and at least four times before and after image data acquisition
2. Attitude data with respect to the local orbit coordinate frame measured by gyros and the star tracker unit with 8Hz; these data are already corrected for several effects (Bouillon et al. 2003)
3. Look direction table for the 12000 CCD elements expressed within the sensor coordinate frame
4. Data used for time synchronization like line sampling period and scene center time.

According to the „SPOT Satellite Geometry Handbook“ (SPOT IMAGE 2002), Lagrange interpolation of the ephemeris data (satellite position and velocity w.r.t. ITRF90 datum) and linear interpolation of the attitude data (Euler angles w.r.t. orbit coordinate frame) are recommended to calculate the exterior orientation for each scan line using scene center time and sampling period for synchronization. After transformation to a local topocentric system (LTS) with a fundamental point located at the center of the image scene, this serves as input for DLR’s processing software. For orthoimage production the exterior orientation is expressed in the Earth Centered Earth Fixed (ECEF) WGS84 Cartesian frame. Details of the mathematical handling are given in Reinartz et al 2006.

4. ORTHOIMAGE GENERATION AND ACCURACY ANALYSIS

To assess the absolute and relative accuracy of the position and attitude data, and to get an estimation of the necessity to improve the ancillary data by bundle adjustment or other methods, orthoimages were derived using an already available DSM.

The inputs for the orthoimage production are the interior orientation (CCD look angles), the six parameters of the exterior orientation for each image line (interpolated from the measured sampling points) and the DSM. For the Bavarian test site the DSM was derived from several ERS 1/2 Tandem pairs, with an accuracy in the order of 5 to 10 meter in flat and hilly terrain and 10 to 50 meter in mountainous terrain (Roth et al. 1998). Therefore the more reliable part of the orthoimages was found north of the foot of the Alps. In the case of Catalonia the reference DEM described in Section 2 was used for the orthoimage generation.

The principle of the orthoimage production is based on the intersection of the actual sensor viewing direction (pointing vector) with the DSM applying the rigorous collinearity equation. The orthoimage processor calculates the object space coordinates within the local topocentric system and then transforms them to the desired map projection of the output image using geodetic transformations (Müller et al. 2003). Bilinear resampling to a 10 m x 10 m grid was performed.

After generation of the two orthoimages, one for each looking direction, without any ground control information, a check of the accuracy using 20 GCPs in Bavaria and 24 GCPs in Catalonia was performed. Table 1 shows the deviations in x and y direction for the orthoimages in comparison to the control points. The result shows that even without any ground control, the absolute georeferencing accuracy of the HRS sensor is better than 20 meter and standard deviation less than one pixel. This was expected, since the values for the absolute pointing accuracy is given by (Bouillon et al. 2003) to about 33 meters with 90% confidence level and the GCP measuring accuracy is typically in the order of half-pixel size (~5 meter, image plotting error), which partly accounts for the standard deviations.

Table 1: Mean values and standard deviations for the difference to the orthoimages of 20 ground control points in meter in Gauss-Krüger coordinate system (Bavaria)

x1, y1 – Coordinates of ground control points

x2, y2 – Coordinates in orthoimage from forward looking

x3, y3 – Coordinates in orthoimage from backward looking

Bavaria	x2 – x1	y2 – y1	x3 – x1	y3 – y1
MEAN	-4,3	5.0	-14.3	11.5
STDV	5.89	7.35	6.23	8.64
Catalonia				
MEAN	-9,90	-16,59	-0,36	-11,16
STDV.	4,64	8,48	5,72	5,23

An interesting behavior shows up when the orthoimage pairs are compared in detail. An automatic matching (see Section 5) of the two pairs of orthoimages revealed that the difference vectors (each a mean value in a 200 x 200 pixel squared area) showed a very homogeneous behavior across the whole image scene, mean length is about 13 m in the Catalonia test site (Fig. 2) and 23 m in the Bavarian test site, with very low standard deviation (~2 m). This systematic behavior, which shows mainly a constant shift between the two images, can be interpreted as the result of a stable relative orientation during the data acquisition time for each single camera, but an unknown constant deviation from the delivered orientation data for both cameras. With respect to the accurate ephemeris data (less than 1 m RMSE), this behavior lead to the assumption that the absolute pointing of the cameras can be improved by introducing the boresight alignment angles ϵ which can be estimated by very few GCPs (2 - 4). This will be investigated in detail in Section 7.

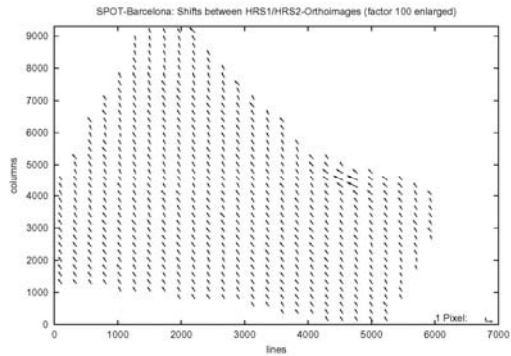


Figure 2: Shifts between the two orthoimages derived from forward and backward looking channels of SPOT HRS (mean values in a regular grid), Catalonia test area

5. IMAGE MATCHING

Matching of the stereo image (or orthoimage) pairs was performed purely in image space with DLR software. Details of this software are described in (Lehner et al. 1992). It relies on a 7-step image resolution pyramid and applies intensity matching in two forms: normalized correlation coefficient for pixel accuracy and subsequent local least squares matching (LLSQM) for refinement to sub-pixel accuracy (for mass points 0.1 to 0.3 pixel standard deviation). Interest points are generated with the Förstner operator and the homologous points are searched for in the other image. These tie points are used as seed points for the subsequent Otto-Chau region growing procedure for dense matching (Heipke et al 1996). The local least squares matching starts with template matrices of 13 x 13 pixels around the seed points with a step of 1 to 3 pixels in each direction. For cross checking and blunder reduction a backward match was performed for all points found. Some more details are described in (Müller et al. 2004).

6. DSM PRODUCTION FROM TWO RAY STEREO DATA

Having the mass points from the matching process as well as the exterior and interior orientation of the camera system from the XML-file, the object space coordinates could be calculated using forward intersection. This was done by least squares adjustment for the intersection of the image rays. The irregular distribution of points in object space after the forward intersection was regularized into an equidistant grid of 15 m (Catalonia) and 25 m (Bavaria) spacing. The interpolation process was performed by a moving plane algorithm (Linder 1999). The resulting DSMs were compared to the reference DEMs, therefore a distinct difference is expected e.g. in forest areas.

6.1. Bavarian test site

In the test site of Bavaria six reference DEMs were available for testing the accuracy (see Fig. 1). Fig. 3 shows as example the derived DSM for test area 06 (size: 50 km x 30 km) east of Munich with moderate terrain, which is the largest of the six test regions.

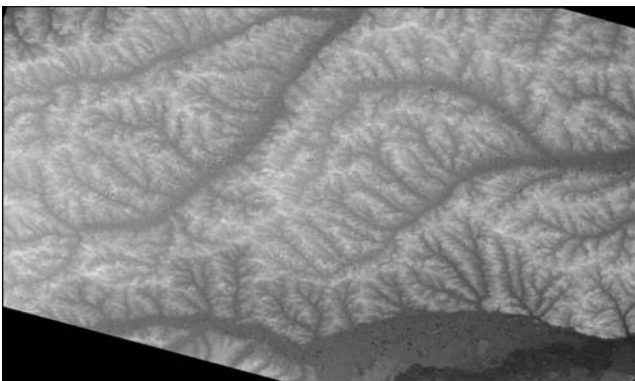


Figure 3. DEM from SPOT-HRS stereo data (region in fig 2).

The comparison of the derived DSM with the reference DEM was performed in several ways. At first only those points, which were matched with high quality were investigated. These points are characterized by very high correlation coefficients. They were compared for all the areas where a reference DEM was available. The result is shown in Table 2; the mean height differences (bias) are due to absolute orientation errors, they seem to be very similar for all reference areas, and can be reduced using the method described in Section 7. The low standard deviations show a very good agreement with the reference DEM.

Table 2: Comparison of height for high quality homologous points in SPOT-DEM and reference DEM

Reference area	Size and Accuracy of Ref-DEM	Mean Height Difference (bias) [m]	STDV [m]	Points [#]
DEM-01, Prien	5 x 5 km, 0.5 m	6.8	2.0	240
DEM-02, Gars	5 x 5 km, 0.5 m	6.2	2.2	184
DEM-03, Peterskirchen	5 x 5 km, 0.5 m	5.6	1.8	261
DEM-04, Taching	5 x 5 km, 0.5 m	4.9	2.0	254
DEM-05, Inzell	10 x 10 km, 5 m	5.7	3.5	458
DEM-06, Vilsbiburg	50 x 30 km, 2-3 m	6.1	3.6	15177

A second comparison was performed by using the regularized SPOT-DSM to perform an area-based analysis. The area related approach of DEM/DSM comparison should distinguish between at least two types of classes (forest and non-forest areas) because of the anticipated discrepancy between terrain models (DEM) and surface models (DSM). The matched points inside a forest area are distributed among different height levels and therefore the standard deviation for the difference of their heights to the reference DEM should be higher. Table 3 shows these results for two of the reference areas in Bavaria.

The mean height differences for non-forest areas are of the same order (around 6 meter) as for the single points in Table 2. The standard deviations are much higher in this area due to lower matching accuracy of the densely matched points and due to interpolation errors in areas where the region-growing matching algorithm could not find enough well correlated points (e.g. low contrast). In the forest areas the mean height differences are about 10 to 12 meter higher due to the surface/terrain model discrepancy. This estimated forest stand heights are actually about 50% of the real tree height in the forest stands, which could be shown in (Reinartz et al 2005). Also the standard deviation is much higher in forest areas as was expected. Fig. 4 shows the difference image of the Laser reference DEM to the SPOT DSM. Forest areas can be seen clearly (brighter grey values) because of the higher mean difference. Also some blunders can be seen in the lower right part of the DSM, which has not been filtered in this case.



Figure 4. Difference DEM (SPOT DEM – Reference DEM): Bright: forest areas and some blunders, the black parts have no value in the reference DEM.

There are many filtering techniques which can be applied to the DSM data. For this paper two techniques were applied: an analysis of the statistics of correlating points (kernels) such as variance and roundness (Förstner operator), excluding points with lower performance, and a median filter with a window size of 3 x 3 pixels (Reinartz 2004). Table 3 shows

that in all cases the filtering leads to significantly lower standard deviations and only little change in absolute differences. The higher change in forest areas is due to a higher error probability of the matching process in these areas. Many falsely matched points were eliminated in the case of the roundness filter and some “height-noise” is well eliminated by the median filtering. Also the mean height differences are lower for the forest areas after filtering since the filters eliminate points with larger height values (Jacobsen 2004). The resulting DSM have a reduced high frequency part (noise), exhibit less errors and are therefore favorable for further applications like 3D-views etc.

Table 3: Comparison of the regularized SPOT-DEM and the reference DEM for selected areas and two surface types (SPOT DEM – Reference DEM)

Reference area	Mean Height Difference [m] <u>non-forest</u> / STDV	Mean Height Difference [m] <u>forest</u> / STDV	Height-difference forest/non-forest
DEM-02	5.9 / 5.6	17.8 / 10.7	11.9
DEM-02 statist. filter	5.7 / 4.8	15.9 / 9.0	10.2
DEM-02 median filter	5.9 / 3.9	15.7 / 9.2	9.8
DEM-06	6.5 / 6.5	19.0 / 9.0	12.5
DEM-06 median filtering	6.2 / 4.2	16.9 / 6.8	10.7

Another possibility of comparison is to look at profiles of the DSM along a given line. In the profiles, the structure of the DSM and its variability can be seen easily. Fig. 5 shows the profiles along the same line for the SPOT DSM and the reference DEM before and after filtering (roundness filter). The rough structure of the profile is very similar to the reference DEM, but there is a high variability in the SPOT DSM without filtering. After filtering the two profiles are more similar to each other, the offset of about 6 m can be seen clearly as well as the signature of a small forest stand around pixel number 32.

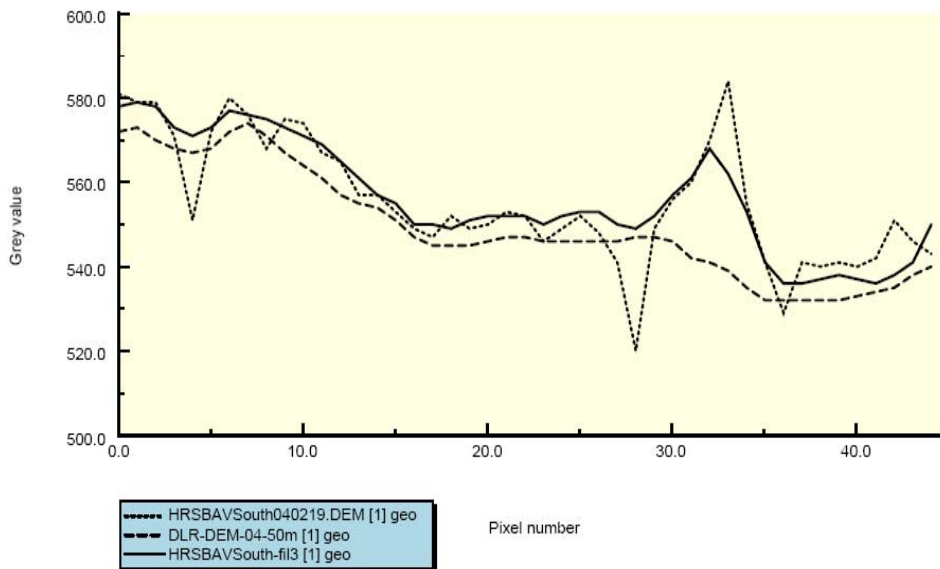


Figure 5. Profiles of SPOT-DEM (dotted), filtered SPOT-DEM (solid) and reference DEM (dashed)

6.2. Catalanian test site

In the Catalanian test site the comparison was possible for larger areas since the reference DEM is available for most of the region covered by the SPOT data. Only an area based comparison is presented. Table 4 shows the mean differences as well as standard deviation and min/max values of the differences for four areas in and around Barcelona. Mean height differences are again very similar in all four cases, and since the orthoimages show also a constant shift (similar to Fig. 2), it gives rise to the assumption that again just a rotation matrix estimated from few GCPs will be necessary to correct the object space coordinates. This will be investigated in the next section.

Table 4: Area-wise comparison of height of SPOT-DEM and reference DEM

Reference area	Size of Area	Mean Height Difference [m]	STDV [m]	Min / Max
Barcelona City	46 km ²	10.0	5.7	-82 / +50
Rural Area	57 km ²	8.2	4.4	-45 / +87
Moderate Mountain	124 km ²	9.0	6.4	-91 / +99
Montserrat (steep mountain)	84 km ²	8.1	15.1	-213 / +245

The standard deviation for HRS-DSM gets higher with more slopes and forest areas. In the case of the mountain range Montserrat, with very steep slopes (some above 45°) the standard deviation and the min/max values become very high. Applying a coarse classification of forest areas, the mean height difference in these areas is only 2-3 meters higher than for other classes. From discussion with local authorities this may be due to less dense forest cover than in the Bavarian case.

7. IMPROVEMENTS BY FEW GCPS

It was shown in Section 4 that even without any ground control, the absolute georeferencing accuracy of the HRS sensor is in the order of one to two pixel and standard deviation less than one pixel. This is in line with the predicted absolute pointing accuracy of about 33 meters with 90% confidence level shown in this issue by (Bouillon et al 2006). By automatic matching of the HRS orthoimages a very homogeneous behavior of the difference vectors was found, which suggests an improvement of the pointing accuracy by few GCPS. The satellite position determination with the DORIS system is in the sub-meter range and variations of georeferencing accuracy is linked to interior orientation changes w.r.t. thermal effects caused by different solar exposure during orbit revolution (latitudinal model) (Bouillon, 2003), which advises corrections of the orientation of the instruments. Selecting different sets of GCPS for estimation of boresight alignment angles (rotational offsets between body and sensor coordinate frame), a series of orthoimages from the forward and backward looking sensors were generated and compared by image matching. The distribution of the GCPS is shown in Fig. 6.

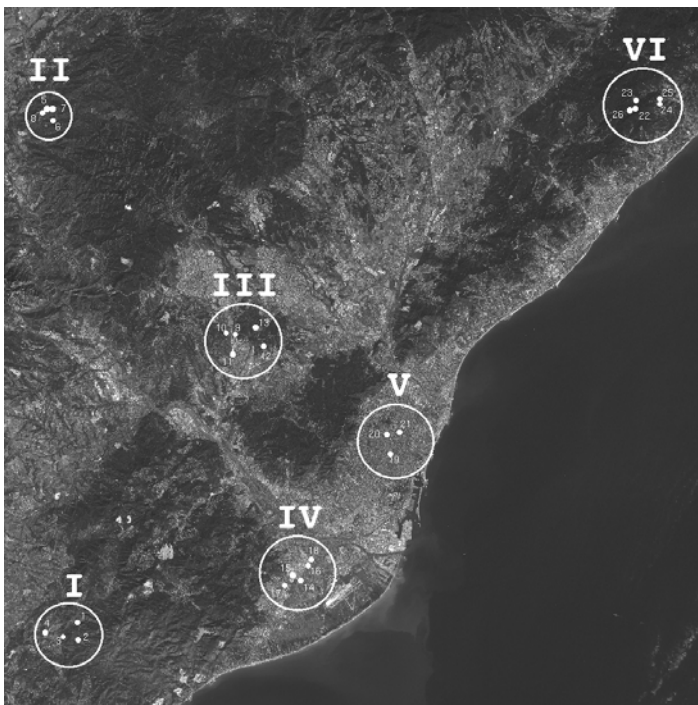


Figure 6 Distribution of GCP groups at Catalonia test site selected from the reference ortho-images. Flight direction is from top to bottom.

The co-registration deviation (Table 5) decreases from 1.3 pixels (=13m) RMSE north/east with no ground control information to 0.3 pixels (=3m) RMSE north/east using all 28 GCPS. More than 100 GCP combinations have been investigated. For the two evaluations of orientation improvement with 3 GCPS in Table 5, the best combination with respect to RMSE at the GCPS after improvement (located in the image regions I/IV/VI of Fig. 6) and a worse

combination (located in region I/V/VI respectively), was chosen. The same was done for two combinations of 4 GCPs (both from the image regions I/IV/V/VI). In both cases the best GCP combinations reached the same co-registration accuracy as the usage of all GCPs. This implies that with 3 to 4 well measured GCPs the same accuracy can be reached as using 28 GCPs, provided they are not too close and distributed over the swath (see Fig. 6). The RMSE values for each of the HRS stereo cameras at the GCPs after improvement is of the magnitude of 0.5 pixels (input data: all GCPs). This seems to be the typical half-pixel image plotting error, caused by the manual measuring process of GCPs in the images (Toutin 2006). The matching of the two orthoimages after orientation improvements led to residuals of only 0.3 pixels. This result indicates that probably the absolute geolocation accuracy is in the order of 0.3 m. It is well worth noticing again that this result can be reached by using 3-4 GCPs and independent improvement of the orientations of the two cameras.

Table 5: Matching results between ortho images from HRS1 and HRS2 before and after improvement, and with different combinations of GCPs (1 pixel = 10m)

HRS1 versus HRS2	Matching Points [#]	RMSE North [pixel]	RMSE East [pixel]	RMSE north/south [pixel]
no GCP	88897	0.49	1.23	1.32
I/VI	94570	0.94	0.23	0.97
I/V/VI	98671	0.59	0.18	0.62
I/IV/VI	103311	0.33	0.15	0.36
I/IV/V/VI	104019	0.42	0.20	0.47
I/IV/V/VI	99956	0.19	0.18	0.27
28 GCPs	111039	0.26	0.15	0.30

With the improved orientation data a new forward intersection and DSM have been calculated for the Catalonia area. It was expected that the bias to the reference DEM is reduced significantly in comparison to Table 4 since the boresight alignment angles should improve the actual look direction for each camera individually. Table 6 shows the results for a combination of 28 and 4 GCPs. The standard deviations are not listed, since they change very little in comparison to the STDV before correction (below 2%, see Table 4) because they depend only little on the better pointing accuracy. The results show that the improvement is in the expected order as was shown through the result of orthoimage matching (Table 5). The positive height bias is partly due to higher values in forest and city areas (surface) in comparison to the reference DEM (ground).

Table 6: Area-wise comparison of height of corrected SPOT-DEM and reference DEM

Reference area	Size of Area	Mean Height Difference [m] 28 GCP	Mean Height Difference [m] 4 GCP
Barcelona City	46 km ²	3.8	4.1
Rural Area	57 km ²	2.1	1.4
Moderate Mountain	124 km ²	3.4	2.6
Montserrat	84 km ²	2.8	0.1
Whole area	1889 km ²	2.5	2.1

8. CONCLUSION

It could be shown that a stereoscopic evaluation of SPOT-HRS data, only using ancillary data (time, position, attitude) and the rigorous method with direct georeferencing, leads to an absolute accuracy of terrain heights in the order of 5 to 10 meter (mean height deviation, bias), with standard deviations of about 2 to 4 meter for single points and 4 to 7 meter for the interpolated DSM in comparison to the reference DEM. The relative accuracy of course depends on terrain steepness and land use classes, since image matching algorithms depend on these image features. The standard deviations are reduced by DEM filtering, which also leads to a smoother DSM. In forest areas the standard deviations are significantly higher and forest heights are estimated to be in the order of 12 meter in Bavaria which is roughly 50% of the real mean tree height. Orthoimages can be derived to an absolute location accuracy of 1 to 2 pixels (10 to 20 meter) without ground control. Using very few (3-4) GCPs and estimating boresight alignment angles it is possible to reach a co-registration accuracy of the individually improved HRS images of less than 3 meter and to reduce the height

bias in the Catalanian case from 9 to 2 meter. This shows that with the very precise ancillary data of the HRS sensor on SPOT 5 it is only necessary to have a few very accurate GCPs to achieve high precision DSMs regarding location and absolute height accuracy. The difficulty in getting many sufficiently accurate and well distributed GCPs stresses once more the benefits of highly accurate exterior orientation measurements.

9. REFERENCES

- Bamler, R., Eineder, M., Kampes, B., Runge, H., Adam, N., 2003. SRTM and beyond: Current situation and new developments in spaceborne SAR and InSAR. Proc. of the ISPRS Workshop High Resolution Mapping from Space, Hanover, Oct. 6-8 October, IPI, Universität Hannover, 6p. (on CD-ROM).
- Bouillon, A., Breton, E., De Lussy, F., Gachet, R., 2003. SPOT5 Geometric Image Quality, Proc. IGARSS 2003, Toulouse, July 21-25 July 8p. (on CD-ROM).
- Bouillon, A., Bernard, M., Gigord, P., Orsoni, A., Rudowski, V., Baudoin, A., 2006. SPOT 5 HRS Geometric Performance. ISPRS Journal of Photogrammetry and Remote Sensing in print
- Heipke, C., Kornus, W., Pfannenstern, A., 1996. The evaluation of MEOS airborne 3-line scanner imagery – processing chain and results. Photogrammetric Engineering and Remote Sensing, Vol. 62, No. 3, pp. 293-299.
- Jacobsen, K., 2004. Analysis of Digital Elevation Models based on Space Information. EARSeL Symposium, Dubrovnik, 2004, 8 p. (on CD-ROM)
- Kornus, W., Alamus, R., Ruiz, A., Talaya, J., 2006. DEM Generation from SPOT-5 3-fold along-track stereoscopic imagery using autocalibration. ISPRS Journal of Photogrammetry and Remote Sensing in print
- Lehner, M., Gill, R.S., 1992. Semi-automatic derivation of digital elevation models from stereoscopic 3-line scanner data. International Archives of Photogrammetry and Remote Sensing 29, (Part B4), pp. 68-75.
- Linder, W., 1999. Geo-Informationssysteme. Springer-Verlag Berlin, Heidelberg, Germany.
- Müller, R., Lehner, M., Müller, R., 2001. Verification of Digital Elevation Models from MOMS-2P data. Proc. ISPRS Workshop “High Resolution Mapping from Space 2001”, Hannover, Germany, 4p. (on CD-ROM)
- Müller, R., Palubinskas, G., Reinartz, P., Schroeder, M., Amann, V., Stätter, R., 2003. From Airborne Digital Raw Data to Image Maps. PFG Photogrammetrie, Fernerkundung, Geoinformation, Germany, 4 (4) pp. 317-326.
- Müller, R., Reinartz, P., Lehner, M., Schroeder, M., 2004. Comparison of the Accuracy of DEM from SPOT HRS two-fold Stereo Data and HRS/HRG three-fold Stereo Data in Barcelona Test Site. International Archives of Photogrammetry, Remote Sensing and Spatial Information Sciences 35 (Part B1), pp. 469-473.
- Rabus, B., Eineder, M., Roth, A., Bamler, R., 2003. The shuttle radar topography mission – a new class of digital elevation models acquired by spaceborne radar. ISPRS Journal of Photogrammetry and Remote Sensing, 57 (4), pp. 241-262.
- Reinartz, P., Lehner, M., Müller, R., Schroeder, M., 2004. Accuracy for DEM and Orthoimages derived from SPOT HRS Stereo Data without using GCP. International Archives of Photogrammetry, Remote Sensing and Spatial Information Sciences 35 (Part B1), pp. 433-438.
- Reinartz, P., Müller, R., Lehner, M., Schroeder, M., 2006. Accuracy Analysis for DEM and Orthoimages derived from SPOT HRS Stereo Data using direct georeferencing. ISPRS Journal of Photogrammetry and Remote Sensing, in print
- Reinartz, P., Müller, R., Hoja, D., Lehner, M., Schroeder, M., 2005. Comparison and fusion of DEM derived from SPOT-5 HRS and SRTM data and estimation of forest heights. Proc. EARSEL Workshop on 3D-Remote Sensing, Porto, 10-11 June 9p. (on CD-ROM).
- Roth, A., Knoepfle, W., Gebhardt, S., Rabus, B., Scales, D., 1998. Evaluation of Interferometric Digital Elevation Models Derived from ERS Tandem Data. ISPRS Commission II Symposium, Cambridge, UK, 13-17 July ISPRS, International Archives of Photogrammetry and Remote Sensing 32 (Part 2), pp. 242-247.
- SPOT IMAGE, 2002. SPOT Satellite Geometry Handbook. S-NT-73-12-SI, Edition 1, Rev. 0, Toulouse, France.
- Toutin, T., Cheng, P., 2001. DEM Generation with ASTER Stereo Data. Earth Observation Magazine, 10 (6), pp. 10-13.
- Toutin, T., 2006. Evaluation of DTMs generated from SPOT-5 in-track HRS and across-track HRG stereo data. ISPRS Journal of Photogrammetry and Remote Sensing, in print